Polym. Bull. (2017) 74:2185–2201
DOI 10.1007/s00289-016-1831-z

ORIGINAL PAPER

Synthesis and characterization of chitosan/poly (vinylpyrrolidone) biocomposite for biomedical application

R. Poonguzhali[1] · S. Khaleel Basha[2] · V. Sugantha Kumari[1]

Received: 5 August 2016 / Revised: 5 October 2016 / Accepted: 11 October 2016 /
Published online: 14 October 2016

Abstract CS/PVP blend membranes at different weight ratios were fabricated using a solution casting method and were characterized by measuring thickness, mechanical properties, water vapour transmission rate (WVTR), and water solubility. Membrane morphology and other characteristics were analysed using scanning electron microscopy, X-ray analysis, DSC, TGA, and ATR-FTIR spectroscopy. SEM and XRD showed that the CS/PVP was homogeneously dispersed in the membrane and the crystallinity decreased with increasing PVP content. The prepared membranes also showed good thermal properties. The strong interaction between the Chitosan and PVP contributed to improvement in the properties of the blend membranes. Membranes with CS/PVP = 1/1 blend ratio of chitosan/PVP showed the most satisfactory Hemolysis, TS, Elongation at break of all tested ratios. The antibacterial activity of the blend membranes was then investigated against Gram-negative *Pseudomonas aeruginosa* and Gram-positive *Staphylococcus aureus*. The PVP concentration contributes to antibacterial effect of the membranes and lower water vapour transmission rate. The in vitro hemolysis test of the membranes showed blood compatibility. These findings suggest that the CS/PVP as a promising material for biomedical application.

Keywords Chitosan · Poly (vinylpyrrolidone) · Solution casting · Hemolysis · Biomedical application

✉ V. Sugantha Kumari
suganthaaux@gmail.com

[1] Department of Chemistry, Auxilium College, Vellore 632 006, India

[2] Department of Chemistry, C. Abdul Hakeem College, Melvisharam 632 509, India

Introduction

The structure and properties of transparent polymeric membranes fabricated from biodegradable polymers have been widely used as wound dressing material, bioadhesive material and drug delivery applications [1–3]. The prepared scaffolds for these applications should be biocompatible, biodegradable, and have good swelling properties to prevent a secondary infection of bacteria [4] as well as good thermal stability. The biopolymers frequently used in the preparation of biomaterials for biomedical applications are gelatin [5], alginate [6], chitosan [7], pectin [8], heparin [9], and cellulose [10]. Among the natural polymers, chitosan occupies a special position due to its abundance, versatility, facile modification and unique properties including biodegradability, biocompatibility, non-toxicity, and antibacterial properties as well ashydrophilicity. This has made chitosan a very useful compound in a wide range of applications in the medical [11], pharmaceutical [12], chemical [13], and agricultural fields [14].

Polyvinyl pyrrolidone (PVP) is a synthetic polymer with excellent water solubility, absorbency, and biocompatibility. The PVP molecule contains a strong hydrophilic component. PVP is also known as povidone or polyvidone consisting of linear 1-vinyl-2-pyrrolidone groups [15]. Biocompatible biopolymers combined with synthetic polymers are of great significance, since it enhances their mechanical, physical, biological and chemical properties, and makes them suitable for complex biological system [16, 17]. Combining chitosan with other polymers has opened a new window of research for altering or tailoring the property of materials [18–20]. To improve chitosan's properties and further diversify its applications, various strategies, such as crosslinking, graft copolymerisation, complexation, chemical modifications, and blending, have been employed. In particular, modification of chitosan by means of blending is an attractive method that has been extensively used for imparting new desirable characteristics to chitosan. This is mainly due to its simplicity, availability of a wide range of synthetic and natural polymers for blending and effectiveness for practical utilisation [21–23].

Blends of CS and PVP are non-toxic, biodegradable, and hydrogels composed of such blends are expected to have high biocompatibility. The CS/PVP systems incorporating varied amounts of these polymers networks were formed and proved advantageous to providing better mechanical, thermal, permeation, biocompatibility, more rigid network structure, cell attachment, and cell viability properties. These properties are very encouraging to these materials in the field of biomedical applications [24].

Our current paper describes a convenient and efficient blending method of CS and PVP to combine the excellent properties of PVP with those of chitosan, and CS/PVP membranes have been developed for biological studies. To study the possibility of use of CS/PVP membrane as biomaterial, a thorough and systematic study of CS/PVP membrane is needed. So in this work, the chemical structure, thermal properties, crystalline, mechanical properties, and morphological studies of CS/PVP membranes were studied by FTIR, TGA, DSC, Tensile studies, and SEM, respectively. The antibacterial activity of CS/PVP membrane was also evaluated.

Experimental

Materials

Chitosan (M_W = 190,000–300,000 g/mol with 80 % deacetylation) extra pure was purchased from Sisco Research Laboratories Pvt. Ltd., Mumbai, India. PVP (M_W = 40,000 g/mol) was purchased from Spectrochemicals Pvt Ltd., Mumbai, India. All other chemicals used were of analytical grade.

Preparation of chitosan/PVP membrane

Chitosan, PVP, and chitosan/PVP blended membranes were individually prepared by solution casting method. One percent of chitosan (w/v) was prepared in one percent aqueous acetic acid, stirred, and filtered to remove the undissolved particles. One percent (w/v) of PVP was prepared by continuous stirring in water. Blend solution to different compositions (i.e., the weight ratios of chitosan and PVP of 1:0, 3:1, 1:1, 1:3, 0:1 (w/w), respectively) were prepared by casting a mixture of the solutions in a respective weight ratio and the membranes were defined as CS/PVP = 1/0, CS/PVP = 3/1, CS/PVP = 1/1, CS/PVP = 1/3, CS/PVP = 0/1, respectively, on a Teflon dish in a dust free environment and left to complete dried in air at room temperature for 48 h. Then, it was kept in a vacuum desiccator till the membrane characterization.

Membrane thickness

Thickness of the membranes was measured using a hand-held Digimatic Micrometer Mitutoyo Corporation, Japan, Model-MDC-1"SB. The average values of five random measurements were taken for each membrane thickness.

Water solubility

The dried membranes were immersed in methanol as a non-solvent for 8 h to remove any residual acetic acid. Then, the samples were taken out and dried in the vacuum oven for 24 h at room temperature. The dried membranes were weighed (W_1), then immersed in distilled water for 8 h, were dried in a vacuum oven for 24 h at room temperature, and then weighed again (W_2). Water solubility was calculated using equation:

$$Ws = 100 \times \frac{W1 - W2}{W1} \quad (1)$$

Water vapour transmission rate

The moisture permeability of the membrane was carried out by measuring the water vapour transmission rate (WVTR) according to the ASTM standard method E 96-95. To measure WVTR, the membranes were mounted at the top of the vial (19 mm

diameter) containing 10 mLs of water. Then, the vials were placed in a desiccator with a saturated solution to ammonium sulfate at 37 °C. The assembly was weighed at regular intervals of time and a weight loss vs. Time plot was constructed. From the slope of the plot, WVTR was calculated as follows:

$$\text{WVTR} = \text{slope} \times {}^{24}/_{A}\left[\frac{\text{g}}{\text{m}^2}/\text{day}\right] \quad (2)$$

where 'A' represents the permeation area of the sample (m^2). Experiments were done in triplicate.

Swelling property

The water sorption capacity of the membranes was determined by immersing the membranes in phosphate buffered solution to pH 7.4 for 8 h at 37 °C. The swollen membranes were removed from predetermined time intervals (1, 2, 3, 4, 5, 6, 7, and 8 h) and immediately weighted with an analytical balance after the removal of excess of water by laying the membranes on a filter paper. The swelling ratio (SR) was calculated using the following equation:

$$\text{Swelling ratio } (\%) = 100 \times (W_t - W_0)/W_0 \quad (3)$$

where W_t and W_0 are the weights of the membranes at time t (swelling state) and at time 0 (dry state), respectively.

Attenuated total reflectance-Fourier transform infrared spectroscopy (ATR-FTIR) spectra

The chemical structure of the prepared membranes was characterized using an attenuated total reflectance Fourier transform (ATR-FTIR) spectrophotometer (Shimadzu IR affinity-1S). Each spectrum was acquired of transmittance mode on a Quest ATR ZnSe crystal cell by accumulation of 250 scans with a resolution of 4 cm^{-1} and a wave number range of 4000–400 cm^{-1}.

Mechanical properties

Each membrane was cut into rectangular strips (4 mm × 10 mm) and the tensile strength (Mpa) and percentage of elongation at break (Mpa) of the membrane samples were measured using MTS Criterion 5 Kn tensile testing system in accordance with standard method ASTM D638-2010 at an extension rate of 50 mm/min. All specimens were drawn at ambient temperature and ultimate tensile strength and were calculated in triplicate using elongation and instantaneously recorded using a computer.

Thermogravimetric analysis (TGA)

The thermal behaviour of the sample was performed with an NETZSCH STA 449F3 thermal gravimetric analyser under a nitrogen atmosphere and at a heating rate of 10 °C/min in the temperature range of 25–600 °C.

Differential scanning calorimetry (DSC)

Differential scanning calorimetry (NETZSCH STA 449F3) was used to analyse the glass transition temperature (T_g), under a nitrogen atmosphere at a heating rate of 10 °C/min.

X-ray diffraction (XRD)

X-ray diffraction patterns of membranes were analysed using an X-ray diffractometer (XRD-Schimadzu XD-D1) with Nickel-filtered Cu–Kα radiation at voltage 30 kV and current of 45 mA.

Scanning electron microscopy (SEM)

The surface morphology of the blends is examined under SEM. This was performed using a scanning electron microscope (SEM), model JEOL 5410LV (Tokyo, Japan), equipped with a system INCA dispersive X-ray detector (Oxford Instruments, Austin, TX, USA), operated at a voltage of 20 kV, and membranes were coated with gold in a sputter coater.

Antibacterial activity

The disc inhibition zone assay was used to qualitatively evaluate the antibacterial activity of the membranes. The antimicrobial testing was carried out with *Staphylococcus aureus* MTCC 1688 and *Pseudomonas aeruginosa* MTCC 3615 purchased from Microbial Type Culture Collection (MTCC), Chandigarh, India.

The bacteria were cultured overnight in the tryptic soybroth (Himedia) and 200 μL of the culture was spread on the Tryptic soy agar plates, followed by placing sample disc of 0.5 cm diameter. The plate was incubated for overnight in the incubator at 37 °C. The plates were observed for the zone of inhibition around the sample disc, and it was measured.

Hemolysis

The haemoglobin released by hemolysis was measured by the optical densities (OD) of the supernatant at 540 nm using an UV–visible Spectrophotometer (Shimadzu UV Visible Spectrophotometer, UVmini-1240). The percentage of hemolysis was calculated according to the following formula:

$$\text{Hemolysis } (\%) = \left(\text{ODs} - \text{OD}_{(-)}\right)/\left(\text{OD}_{(+)} - \text{OD}_{(-)}\right) \times 100 \qquad (4)$$

where OD_S is the optical density of the sample, $\text{OD}_{(-)}$ is the optical density of negative control, and $\text{OD}_{(+)}$ is the optical density of positive control.

Statistical analysis

All the experiments were performed in triplicate, and Student's t test was performed to determine that the statistical significance $p < 0.05$ was considered statistically significance.

Results and discussion

Membrane appearance and thickness

All the prepared membranes were transparent. As shown in Fig. 1, CS/PVP = 1/0 and CS/PVP = 3/1 membranes were slightly yellowish colour, but as the fraction of PVP increased, the CS/PVP = 1/1 and CS/PVP = 1/3 membranes became colourless. Thickness of the membranes is shown in Table 1 and had ranges from 26.42 ± 1.3 to 43.63 ± 1.8 μm. The thickness of the CS/PVP = 3/1 was significantly higher than the normal thickness of chitosan membrane. CS/PVP = 0/1 has the minimum value of 26.42 ± 1.3 and CS/PVP = 1/3 has thickness of 38.17 ± 0.8.

Water solubility

PVP is a water soluble polymer, while chitosan is soluble in dilute acidic solution (pH < 6.5) but insoluble in pure water. Owing to the semi crystalline structure of

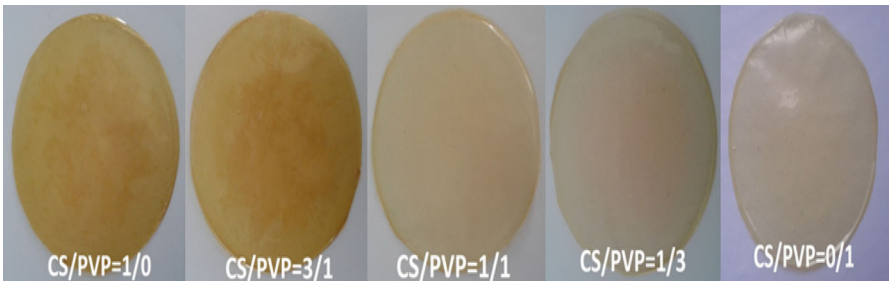

Fig. 1 Images of CS/PVP = 1/0, CS/PVP = 3/1, CS/PVP = 1/1, CS/PVP = 1/3, and CS/PVP = 0/1 membranes

Table 1 Thickness of CS/PVP = 1/0, CS/PVP = 3/1, CS/PVP = 1/1, CS/PVP = 1/3, and CS/PVP = 0/1 membranes

Membrane	Thickness (μm)
CS/PVP = 1/0	40.94 ± 2.7
CS/PVP = 3/1	43.63 ± 1.8
CS/PVP = 1/1	32.82 ± 2.4
CS/PVP = 1/3	38.17 ± 0.8
CS/PVP = 0/1	26.42 ± 1.3

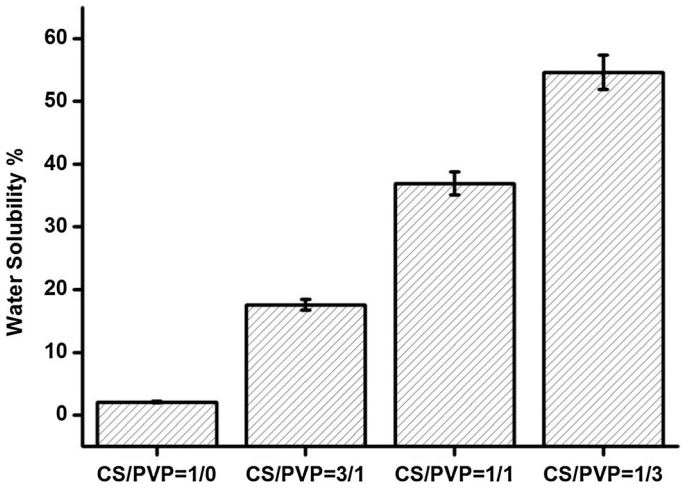

Fig. 2 Solubility of CS/PVP = 1/0, CS/PVP = 3/1, CS/PVP = 1/1, and CS/PVP = 1/3 membranes

chitosan with extensive hydrogen bonding, it will be insoluble in water. The results with water solubility of CS/PVP blend membranes are shown in Fig. 2. The solubility of CS/PVP = 1/0, CS/PVP = 3/1, CS/PVP = 1/1, and CS/PVP = 1/3 were 2.07 ± 0.8, 17.57 ± 0.7, 36.92 ± 1.0, and 54.63 ± 1.0 %, respectively. According to the results, water solubility of the membranes increased with increasing PVP content. Although the membranes maintained the original shape after being immersed in water for 8 h at room temperature, but the weight loss of the blended membranes was increased by decrement of the blend ratio, (e.g., CS/PVP = 1/3 membrane highly dissolved in water, i.e., 54.63 ± 1.0 %). Thus, the blend ratios have a significant effect on solubility in water.

Water vapour transmission rate

Water vapour transmission rate is the most significant factor in determining the suitability of the biomedical membrane for a particular wound. An ideal wound dressing should control water loss from the wound at an optimal rate. As shown in Fig. 3, WVTR was significantly affected by the ratio of the polymers from 1986 ± 22 g/m^2/day for CS/PVP = 1/0 membrane to 2412 ± 66 g/m^2/day for CS/PVP = 0/1 membrane. The water vapour transmission rate of the CS/PVP membranes was 1986–2412 g/m^2/day which is very close to the ideal value for wound dressing. Compared to water vapour transmission rate of different ratios of CS/PVP blend membranes, CS/PVP = 1/1(2128 ± 44 g/m^2/day) could control water evaporation loss at an appropriate rate to maintain a moisture environment.

As suggested by Hashemi and Hualin Wang [25, 26], WVTR through a hydrophilic membrane depends on solubility and diffusivity of water molecules in the membrane. Water vapour transmission rate of membrane was significantly increased with added PVP into chitosan.

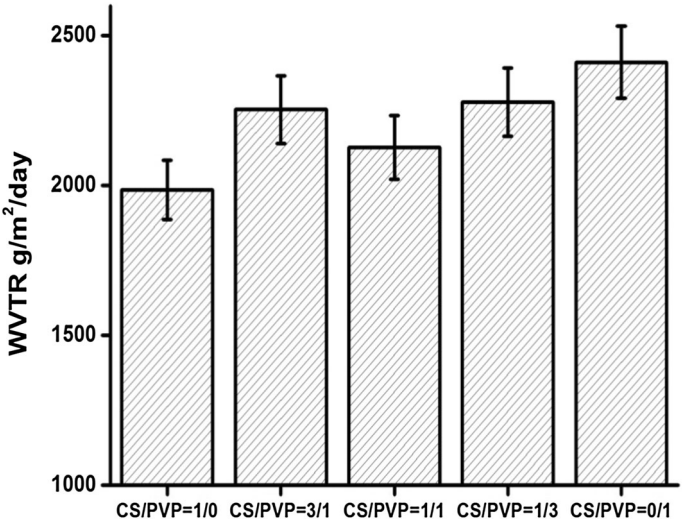

Fig. 3 Water vapour transmission rate of CS/PVP = 1/0,CS/PVP = 3/1,CS/PVP = 1/1, CS/PVP = 1/3, and CS/PVP = 0/1 membranes

Swelling property

Water uptake ability of a biomaterial is an important factor of cell seeding which affects distribution of cell suspension throughout the material and transfer efficiency of oxygen and nutrient. Figure 4 shows that the sample of the highest degree of swelling will have the highest surface area/volume ratio. The CS/PVP = 1/1 membrane shows the highest swelling ratio when compared with other ratios. In Fig. 4, apparent swelling in CS/PVP = 1/3 decreases with time, certainly because part of PVP is solubilized. This can be explained, because PVP reduces the crystallinity of the blend. In addition, PVP has a higher affinity of water, and it makes that the membrane with chitosan swell with greater extent. It can be easily seen from Fig. 4 that the membrane attains equilibrium state after certain period of time. The water absorption behaviour of chitosan was expected due to the amino and hydroxyl groups [27]. This high swelling property of the membrane could be due to hydrophilic nature of materials.

Attenuated total reflectance-Fourier transform infrared spectroscopy (ATR-FTIR) spectra

ATR-FTIR is a technique to probe the extent of chemical interactions between two polymers. Figure 5 shows the ATR-FTIR spectra of CS/PVP = 1/0, CS/PVP = 3/1, CS/PVP = 1/1, CS/PVP = 1/3, and CS/PVP = 0/1 membranes. The spectrum of CS/PVP = 1/0 (chitosan membrane) shows peaks at wavenumber 1639 and 1554 cm^{-1} which indicates the presence of amide I and amide II bands. The clear absorption spectra present at 1026 cm^{-1} shows the presence of –C–N group. The

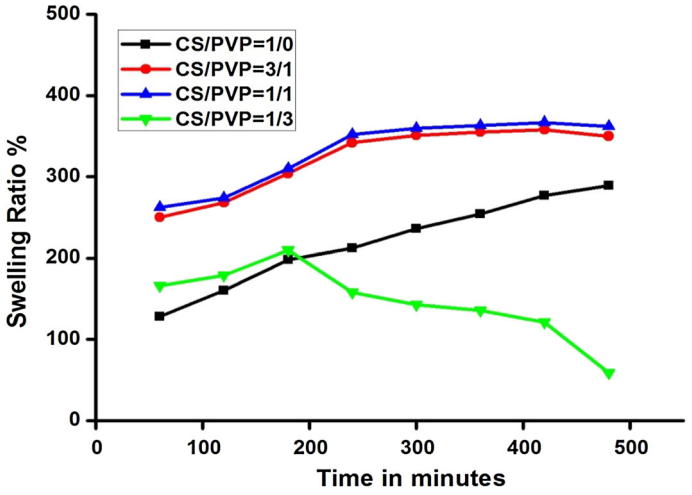

Fig. 4 Swelling studies of CS/PVP = 1/0, CS/PVP = 3/1, CS/PVP = 1/1, and CS/PVP = 1/3 membranes

broad peak obtained at 3300 cm^{-1} reveal that the presence of both –OH and $–NH_2$ groups in chitosan membrane.

The absorption peak at 1643 cm^{-1} for pure PVP corresponding to amide and also corresponding to the –C=O and –C–N group. PVP shows an amide carbonyl band of 1643 cm^{-1}, which is higher than that observed in pure chitosan. The three CS/PVP blends of different weight ratio (CS/PVP = 3/1, CS/PVP = 1/1, CS/PVP = 1/3) showed distinct –C=O group absorption spectra at 1646, 1647, 1649 cm^{-1}, respectively, and –OH absorption for chitosan in the blend shifted downwards in frequency from about 3433 cm^{-1} to about 3251, 3084, and 2954 cm^{-1}. The shifting of the characteristic peaks of chitosan to higher frequencies of –C=O and lower frequencies of –OH suggesting an interaction between chitosan and PVP through hydrogen bonds as the PVP weight ratio increased. This suggests the formation of intermolecular hydrogen bonding with the molecules in the blended membranes.

Mechanical properties

The membranes suitable for wound dressing should preferably strong but flexible. The influence of chitosan and PVP on the mechanical properties of prepared membrane was evaluated. Figure 6a, b shows the results of tensile strength and elongation at break of CS/PVP membrane with different ratios. For CS/PVP = 1/0 membrane, although it had a high value of tensile strength (38 ± 1.0 MPa), it only had a very low elongation at break value (23.0 MPa). When adding PVP into CS/PVP = 1/0 membrane, its elongation at break could be increased greatly and tensile strength values decreased compared with that CS/PVP = 1/0 membrane. The tensile strength for CS/PVP = 3/1, CSPVP = 1/1, and CS/PVP = 1/3 membranes was 37 ± 1.0; 27 ± 1.0; and 16 ± 1.0 MPa, respectively. Correspondingly, the elongation at break for these membranes was 38 ± 1.0, 52 ± 1.0, 46 ± 1.0 MPa,

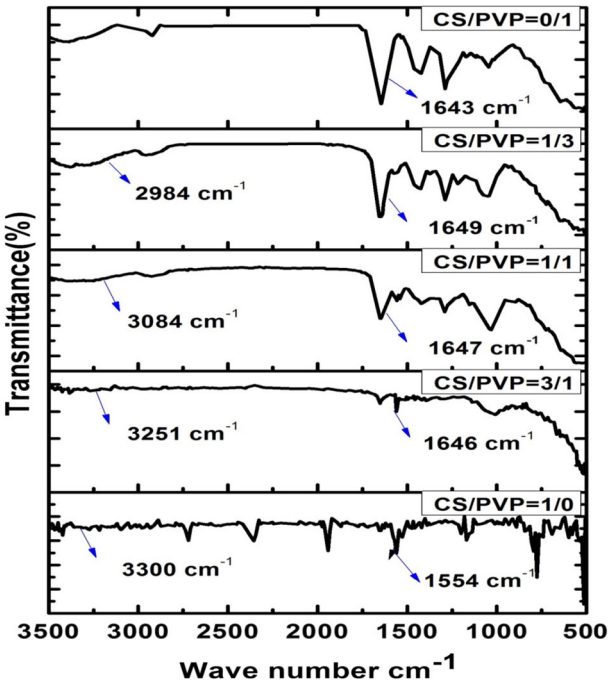

Fig. 5 ATR-FTIR of CS/PVP = 1/0, CS/PVP = 3/1, CS/PVP = 1/1, CS/PVP = 1/3, and CS/PVP = 0/1 membranes

respectively. Generally, increasing the quantity of PVP decreased the strength of the membrane, but the flexibility of the blended membrane increases. This could be due to rigid and fragile nature of PVP. Even though the strong hydrogen bonding formed between the CS and PVP has been proved from ATR–FTIR, the strength of membrane was decreased and elongation at break increased. Overall, the results of tensile test and elongation at break suggested that adding PVP into CS membrane could greatly modify CS membrane's flexibility.

Thermogravimetric analysis (TGA)

The thermal stability and thermal decomposition of prepared blended membranes were investigated by TGA and given in Fig. 7. The TGA curves of CS/PVP = 1/0 and CS/PVP = 0/1 show a single weight loss stage ranging from 250° to 310° and 410° to 470 °C due to water absorption followed by a final decomposition at 550 °C [28]. The TGA curve of blended membranes CS/PVP = 3/1, CS/PVP = 1/1, and CS/PVP = 1/3, Fig. 7 shows two weight losses stages at 220 °C and 230°–250 °C. The first weight loss stage may have corresponded to the degradation of the side chain followed by the main chain degradation of the polymer. Hence, from the thermal stability studies, it can be said that CS/PVP = 1/1 is having more decomposition rate.

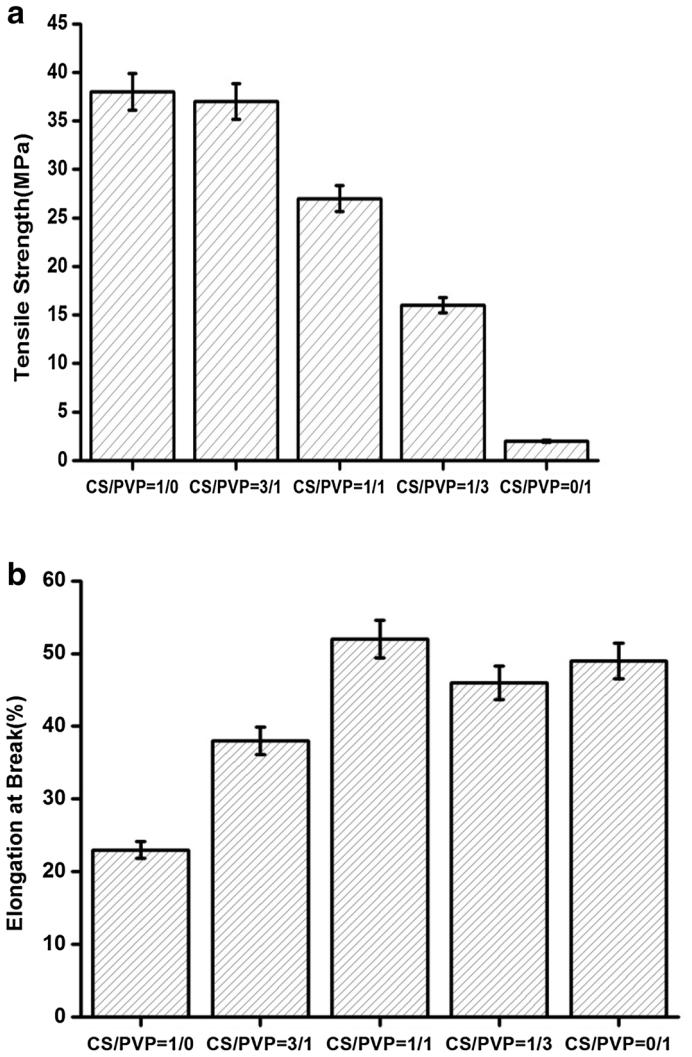

Fig. 6 **a** Tensile property of CS/PVP = 1/0, CS/PVP = 3/1, CS/PVP = 1/1, CS/PVP = 1/3, and CS/PVP = 0/1 membranes. **b** Elongation at break of CS/PVP = 1/0, CS/PVP = 3/1, CS/PVP = 1/1, CS/PVP = 1/3, and CS/PVP = 0/1 membranes

Differential scanning calorimetry (DSC)

Differential scanning calorimetry (DSC) was used to assess the miscibility of Chitosan and PVP blended membranes. DSC thermogram of chitosan, PVP, and CS/PVP blended membranes are shown in Fig. 8. The DSC curves of the CS/PVP membrane reveal that the CS and PVP in the membrane mixed uniformly and their compatibility was good.

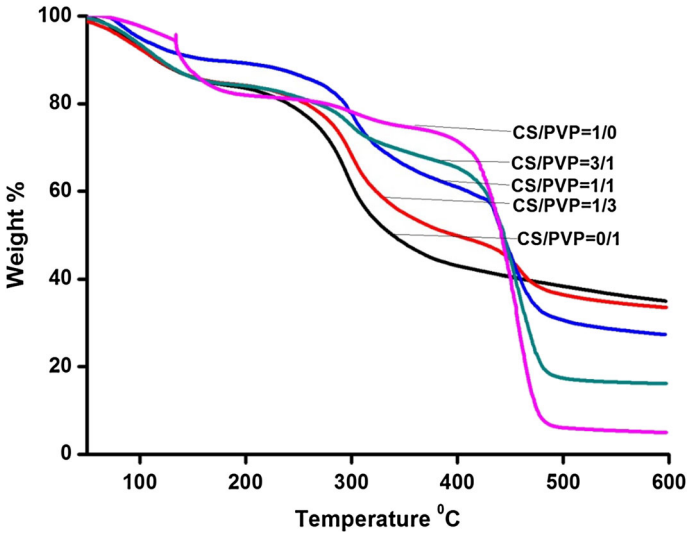

Fig. 7 TGA of CS/PVP = 1/0, CS/PVP = 3/1, CS/PVP = 1/1, CS/PVP = 1/3, and CS/PVP = 0/1 membranes

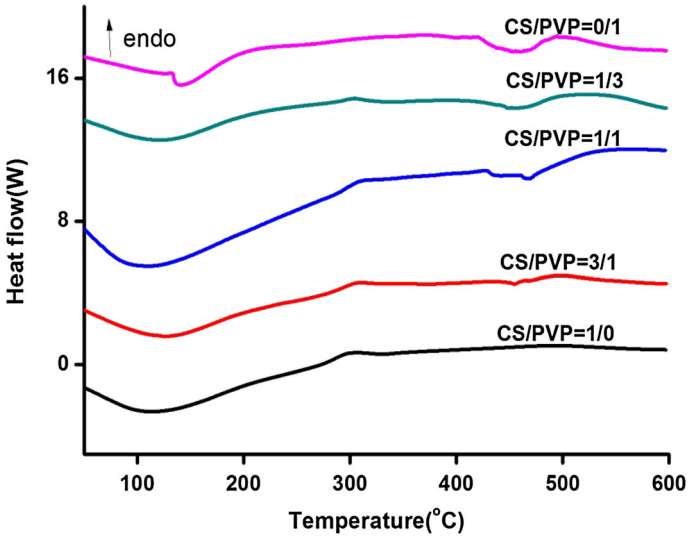

Fig. 8 DSC thermogram of CS/PVP = 1/0, CS/PVP = 3/1, CS/PVP = 1/1, CS/PVP = 1/3, and CS/PVP = 0/1 membranes

The glass transition temperature for chitosan could be estimated to be 120 °C depends on deacetylation degree of chitin. The Tg value of PVP also depends on its molecular weight [29] which may vary from 154 to 174 °C. In Fig. 8, it shows the Tg value of PVP will be about 170 °C. It can be seen that with the content of PVP

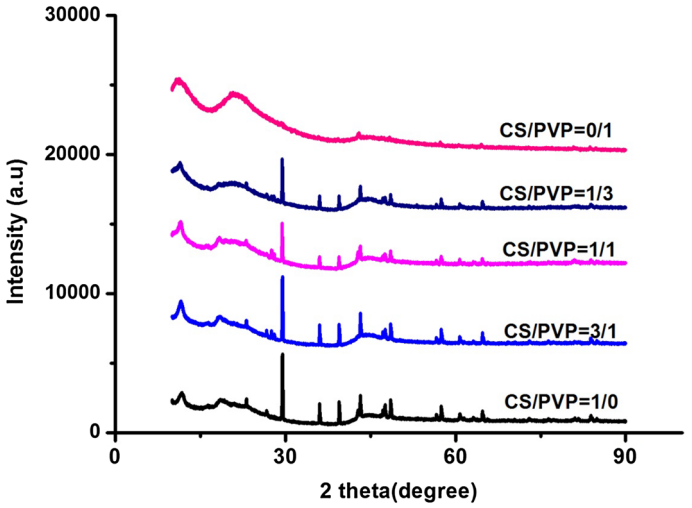

Fig. 9 XRD of CS/PVP = 1/0, CS/PVP = 3/1, CS/PVP = 1/1, CS/PVP = 1/3, and CS/PVP = 0/1 membranes

increasing to the CS/PVP membranes, the curve became larger and sharper. There was a peak at around 105 °C in DSC thermogram of CS/PVP = 1/0, CS/PVP = 3/1, CS/PVP = 1/1, and CS/PVP = 1/3 membranes. These may be attributed to the large influence of sorbed moisture due to the hydrophilic nature of the material.

X-ray diffraction (XRD)

The XRD pattern of CS/PVP = 1/0, CS/PVP = 3/1, CS/PVP = 1/1, CS/PVP = 1/3, and CS/PVP = 0/1 blend membranes are shown in Fig. 9. The X-ray diffractogram of chitosan shows two crystalline peaks at 2θ equals to 29.4° and 19.8°, while CS/PVP = 0/1 shows two broad peaks equals to 14°θ and 24°θ which shows amorphous nature of PVP. Whereas the X-ray diffraction of blended membranes CS/PVP = 3/1, CS/PVP = 1/1, and CS/PVP = 1/3 shows peak at 29.2°, 29.0°, and 28.8°, which can be attributed to the crystalline nature of the membrane. Chitosan shows two crystalline peaks because of presence of –OH and $–NH_2$ groups in the chitosan structure, which could form stronger hydrogen bonds, so that the molecules easily form crystalline regions [30]. XRD crystallization intensity of blended membranes decreased after the addition of PVP to chitosan. The intensity of the peak decreased as PVP concentration increased, and due to enhancing complexation between chitosan and the PVP blended membranes. The significant shift in the diffraction peaks indicated that there was a molecular miscibility and interaction between the components [31]. The XRD results, thus, provided supporting evidence of the FTIR result that some specific chemical interaction between CS and PVP existed in the blend membranes.

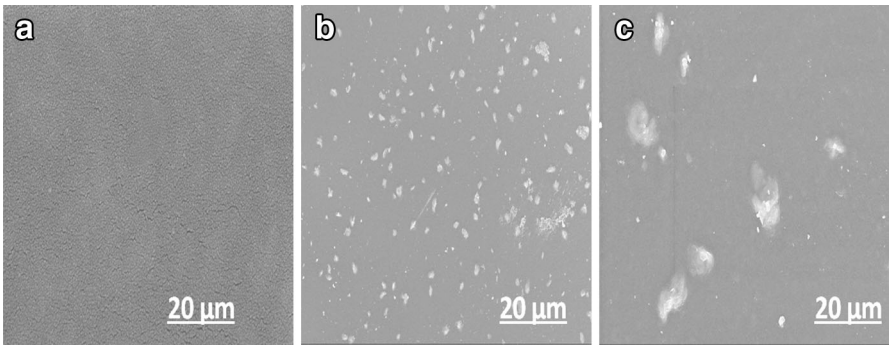

Fig. 10 SEM images of **a** CS/PVP = 1/1, **b** CS/PVP = 3/1, and **c** CS/PVP = 1/3 membranes

Scanning electron microscopy (SEM)

The membranes of CS/PVP blend were examined by scanning electron microscopy to verify the compatibility between chitosan and PVP molecules. In Fig. 10a, the membrane of CS/PVP = 1/1 showed a smooth and homogeneous morphology, suggesting high miscibility and blend homogeneity between chitosan and PVP. The smooth morphology is closely related to the semicrystalline nature of the polymer.

Figure 10b, c shows an irregular particle appearance owing to the polymer membrane formation, indicating the partial compatibility between the two polymers at certain weight ratios. When the quantity of chitosan and PVP exceeded, 75 % incompatibility occurred in the prepared membranes.

Antibacterial activity

The antibacterial activity of the CS/PVP membranes was examined by measuring the inhibition zones of *S. aureus* and *P. aeruginosa* cells, as shown in Table 2. Membranes of CS/PVP = 1/1 and CS/PVP = 3/1 showed better antibacterial activity than CS/PVP = 1/0 and CS/PVP = 3/1 membranes. The effect of exposure to the Gram-positive *S. aureus* and the Gram-negative *P. aeruginosa* to CS/PVP = 1/1 and CS/PVP = 3/1, which caused a decrease in viable cell counts of

Table 2 Antibacterial activity of CS/PVP = 1/0, CS/PVP = 3/1, CS/PVP = 1/1, and CS/PVP = 1/3 membranes

Samples	Zone of inhibition (mm)	
	S. aureus (MTCC 1688)	*P. aeruginosa* (MTCC 3615)
CS/PVP = 1/0	5.7 ± 0.9	5.2 ± 0.8
CS/PVP = 3/1	8.3 ± 0.3	7.8 ± 0.2
CS/PVP = 1/1	10.9 ± 0.7	11.4 ± 0.3
CS/PVP = 1/3	2.8 ± 0.6	4.3 ± 0.4

Data are presented as the mean ± SD ($n = 4$, $P < 0.05$)

both Gram-positive and Gram-negative bacteria. It was observed that chitosan was effective against decreasing the viable cell count of *S. aureus* (inhibition zone diameter 5.7 ± 0.9 mm for CS/PVP = 1/0), and *P. aeruginosa* (inhibition zone diameter 5.2 ± 0.8 mm for CS/PVP = 1/0). In addition, CS/PVP = 1/1 had inhibitory activity on *S. aureus* (inhibition zone diameter = 10.9 ± 0.7 mm), and *P. aeruginosa* (inhibition zone diameter = 11.4 ± 0.3 mm) than CS/PVP = 1/3 with an inhibition zone diameter 2.8 ± 0.6 and 4.3 ± 0.4 mm of *S. aureus* and *P. aeruginosa*, respectively. It was obvious that increasing the percentage of PVP caused lower inhibition of viable cell counts of both *S. aureus* and *P. aeruginosa,* i.e., CS/PVP = 1/3 has very low antibacterial activity. Generally, the antibacterial activities of the tested membranes were stronger against *S. aereus* and *P. aeruginosa*. This inhibition zone against different bacterial cultures proves that CS/PVP = 1/1 material had an excellent antibacterial activity. This may be attributed that the interaction between positively charged chitosan and negatively charged microbial cell membrane. The intermediate was mediated by the electrostatic forces between the protonated $-NH_3^+$ groups of chitosan and the electronegative charges on microbial cell surface. This electrostatic interaction results in dual interferences by promoting changes in the membrane wall permeability properties, thus provoking internal osmotic imbalances, which inhibit the growth of the microorganisms, by the peptidoglycans hydrolysis in the microorganism wall leading to the leakage of intracellular electrolytes, such as potassium ions, and other low molecular weight proteinaceous constituents (e.g., protein, nucleic acid, glucose, and lactate hydrogenase). In our study, there is less but growth of bacteria is observed in blended membranes, it depends on the PVP content. This shows the bacteriostatic not bactericidal properties of the blended scaffolds.

Hemolysis

Hemolysis assay was carried out to study the blood compatibility of membrane. The in vitro blood compatibility of the prepared CS/PVP membranes was investigated using a haemolytic test, as shown in Fig. 11. Generally, smaller the hemolysis ratio value, better the blood compatibility of the biomaterial.

According to the classification of haemolytic tendency towards polymeric materials, [32] it is clear about the figure the hemolysis (%) values vary from the range 0.6–1.92 %, which indicate for a good compatibility of the membranes, and non-hemolysis materials were found. These results can be explained by the fact that both PVP and CS are highly hydrophilic and was in acceptable range of hemocompatibility.

Conclusion

Novel polymer membranes of CS/PVP of different ratios were prepared by solution casting method. CS/PVP membranes physical, chemical, crystalline, thermal properties, and morphologies were studied by thickness, solubility, water vapour

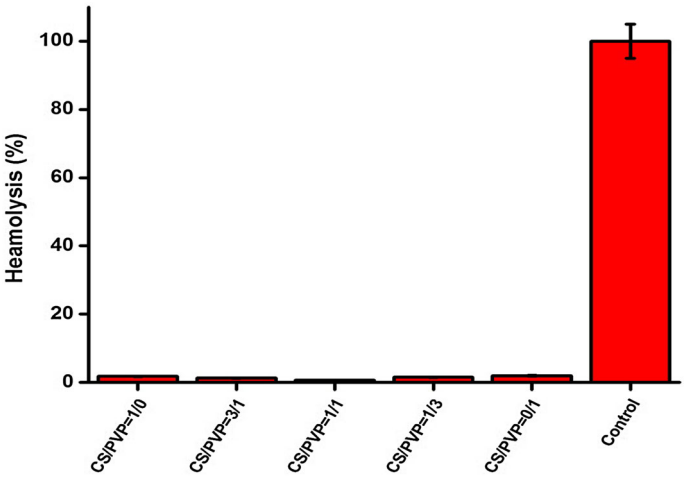

Fig. 11 Hemolysis of CS/PVP = 1/0, CS/PVP = 3/1, CS/PVP = 1/1, CS/PVP = 1/3, CS/PVP = 0/1, and control membranes

transmission rate, ATR-FTIR, XRD, TGA DSC, and SEM. CS and PVP had strong interactions with each other by forming hydrogen bonds between them confirmed by ATR-FTIR. Addition of PVP increases the tensile strength and degree of swelling of CS/PVP blend membranes. The mechanical properties of CS/PVP composite blend membranes were found to be higher with 1:1 CS/PVP. TGA and DSC analysis confirmed the good thermal properties of blend membranes. The antibacterial experiment indicated that CS/PVP blends had good activity against the Gram-negative (*P. aeruginosa*) and Gram-positive (*S. aureus*) bacteria. Hemolysis test showed that the prepared CS/PVP = 1/1 ratio is having optimal hemocompatible nature. These properties can make CS/PVP blend membranes a potential material for the synthesis of a new class of bio-composites and might be used as wound dressing purpose.

References

1. Archana D, Singh BK, Dutta J, Dutta PK (2014) Chitosan- PVP-nano silver oxide wound dressing: in vitro and in vivo evaluation. Int J Biol Macromol 10:10–55
2. Lim JI, Kang MJ, Lee W-K (2014) Lotus-leaf-like structured chitosan–polyvinyl pyrrolidone films as an anti-adhesion barrier. Appl Surf Sci 320:614–619
3. Maria JA, Oliveira MJ, Valdir S (2015) Drug delivery glucantime in PVP/chitosan. Membranes 85:4–9
4. Archana D, Dutta J, Dutta PK (2013) Evaluation of chitosan nano dressing for wound healing: characterization, in vitro and in vivo studies. Int J Biol Macromol 57:193–203
5. Yang Y, Tang H, Kowitsch A (2014) Novel mineralized heparin–gelatin nanoparticles for potential application in tissue engineering of bone. J Mater Sci Mater Med 25:669–680
6. Sapir Y, Kryukov O, Cohen S (2011) Integration of multiple cell-matrix interactions into alginate scaffolds for promoting cardiac tissue regeneration. Biomaterials 32:1838–1847
7. Lee JS, Baek SD, Venkatesan J (2014) In vivo study of chitosan natural nano hydroxyapatite scaffolds for bone tissue regeneration. Int J Biol Macromol10:1–24

8. Takei T, Sugihara K, Yoshida M, Kawakami K (2013) Injectable and biodegradable sugar beet pectin/gelatin hydrogels for biomedical applications. J Biomater Sci Polym Ed 10:1333–1342
9. Nie J-J, Zhao W, Hao H, Bingran Y, Fujian X (2016) Controllable heparin based comb copolymers and their self-assembled nanoparticles for gene delivery. Acs Appl Mater Interfaces 10:1–41
10. Nakasone K, Ikematsu S, Kobayashi T (2015) Biocompatibility evaluation of cellulose hydrogel film regenerated from sugarcane bagasse waste and its in vivo behavior in mice. Ind Eng Chem Res 10:1–29
11. Rodríguez-Vázquez M, Vega-Ruiz B, Ramos-Zúñiga R (2015) Chitosan and its potential use as a scaffold for tissue engineering in regenerative medicine. Bio Med Res Int 15:1–15
12. Zhang J, Xia W, Liu P (2011) Chitosan modification and pharmaceutical/biomedical applications. Mar Drugs 8:1962–1987
13. Qian L, Zhang H (2012) Green synthesis of chitosan-based nanofibers and their applications. Green Chem 10:1–8
14. El Hadrami A, Adam LR (2010) Chitosan in plant protection. Mar Drugs 8:968–987
15. Sanders WC (2015) fabrication of polyvinylpyrrolidone micro-/nano structure utilizing microcontact printing. J Chem Educ 10:1–5
16. Ramadass SK, Perumal S, Gopinath A (2014) Sol−gel assisted fabrication of collagen hydrolysate composite scaffold: a novel therapeutic alternative to the traditional collagen scaffold. ACS Appl Mater Interfaces 6:15015–15025
17. Mansur HS, Ezequiel de S. Costa, Alexandra AP, Mansur (2009) Cytocompatibility evaluation in cell-culture systems of chemically crosslinked chitosan/PVA hydrogels. Mater Sci Eng C 29:1574–1583
18. Velásquez-Cock J, Ramírez E, Betancourt S (2014) Influence of the acid type in the prouction of chitosan films reinforced with bacterial nanocellulose. Int J Biol Macromol 69:208–213
19. Dash M, Chiellini F, Ottenbrite RM, Chiellini E (2011) Chitosan—a versatile semi-synthetic polymer in biomedical Applications. Prog Polym Sci 36:981–1014
20. Stoica P, Chifiriuc MC (2015) Fabrication, characterization and bioevaluationof novel antimicrobial composites based on polycaprolactone, chitosan and essential oils. Rom Biotechnol Lett 20:10521–10533
21. Mehta A, Kanungo I, RaghavaRao J, Nishad Fathima N (2015) Micro environmental changes in collagen/polyvinyl alcohol blends in the presence of ionic liquid: a spectroscopic analysis.J. Bioact Compat Polym 10:1–11
22. Thankam FG, Muthu J, Sankar V (2013) Growth and survival of cells in biosynthetic poly vinyl alcohol–alginate IPN hydrogels for cardiac applications. Colloids Surf B.107:137–145
23. Abdelrazek EM, Elashmawi IS, Labeeb S (2010) Chitosan filler effects on the experimental characterization, spectroscopic investigation and thermal studies of PVA/PVP blend films. Phys B 405:2021–2027
24. Sakurai K, Maegawa T, Takahashi T (2000) Glass transition temperature of chitosan and miscibility of chitosan/poly (*N*-vinyl pyrrolidone) blends. Polymer 41:7051–7056
25. Doulabi AH, Mirzadeh H (2013) Chitosan/polyethylene glycol fumarate blend film: physical and antibacterial properties. Carbohydr Polym 92:48–56
26. Wang H, Zhang R, Zhang H, Jiang S (2015) Kinetics andfunctionaleffectiveness of nisin loaded antimicrobial packaging film based on chitosan/poly (vinyl alcohol). Carbohydr Polym 127:64–71
27. Costa-Júnior ES, Barbosa-Stancioli EF, Mansur AA (2009) Preparation and characterization of chitosan/poly (vinyl alcohol) chemically crosslinked blends for biomedical applications. Carbohydr Polym 76:472–481
28. Dhawade Prerna P, Jagtap Ramanand N (2012) Characterization of the glass transition temperature of chitosan and its oligomers by temperature modulated differential scanning calorimetry. Pelagia Res Library 3:1372–1382
29. Haaf F, Sanner A (1985) Polymers of N-vinylpyrrolidone: synthesis, characterization and uses. Polym J 17:143–152
30. Duan W, Chen C, Jiang L (2008) Preparation and characterization of the graft copolymer of chitosan with poly[rosin-(2-acryloyloxy)ethyl ester]. Carbohydr Polym 73:582–586
31. Zhong Q-P, Xia W-S (2008) Physicochemical properties of edible and preservative films from chitosan/cassava starch/gelatin blend plasticized with glycol. Food Technol Biotechnol 46:262–269
32. Higa OZ, Rogero SO, Machado LDB, Mathor MB (1999) Biocompatibility study for PVP wound dressing obtained in different conditions. Radiat Phys Chem 55:705–707